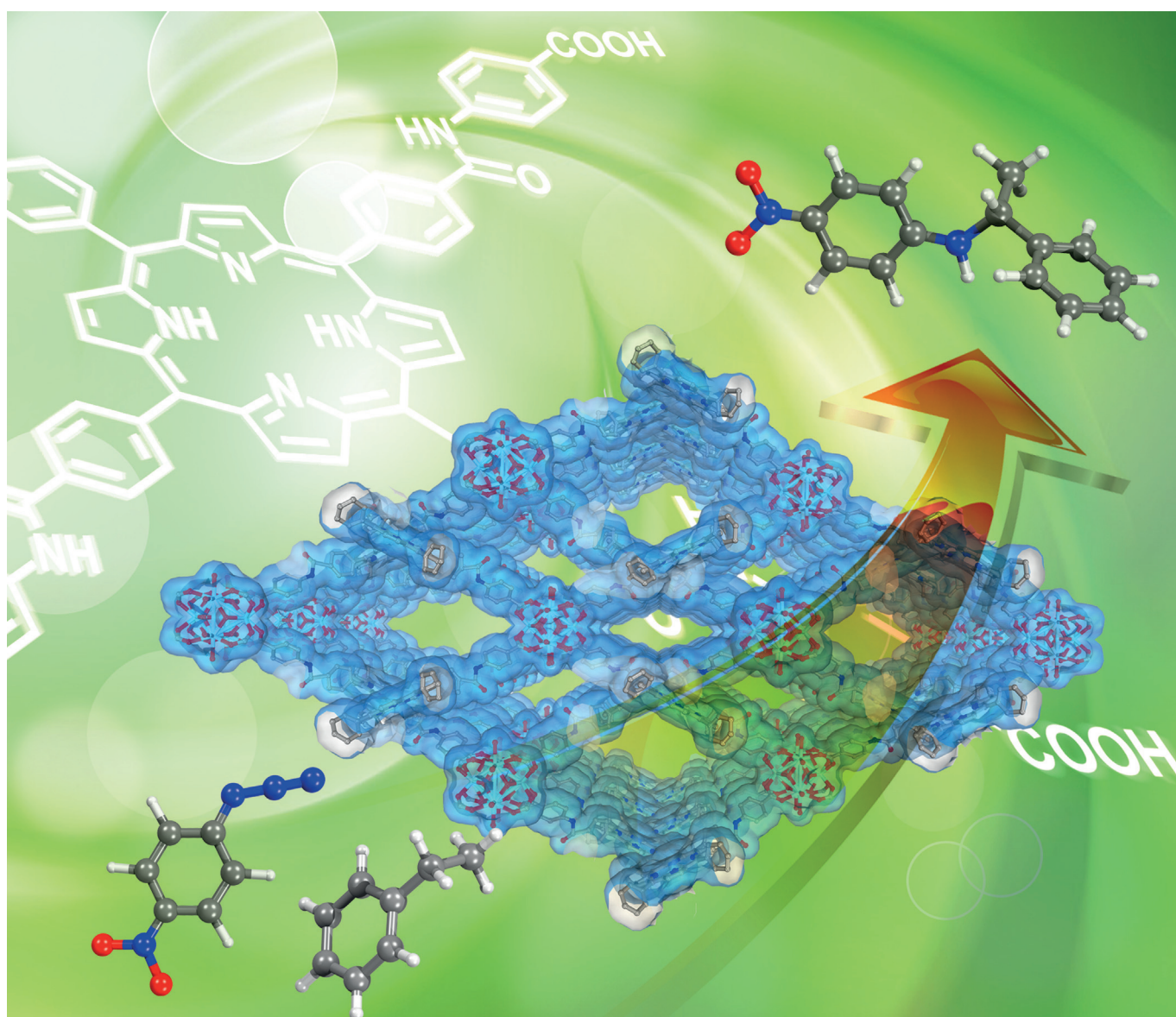


## Metal–Organic Frameworks

## Highly Stable Mesoporous Zirconium Porphyrinic Frameworks with Distinct Flexibility

Lei Xu,<sup>[a]</sup> Yan-Ping Luo,<sup>[b]</sup> Lin Sun,<sup>[a]</sup> Yan Xu,<sup>[c]</sup> Zhong-Sheng Cai,<sup>[a]</sup> Min Fang,<sup>\*,[b]</sup>  
Rong-Xin Yuan,<sup>[b, d]</sup> and Hong-Bin Du<sup>\*,[a]</sup>



**Abstract:** The construction of highly stable metal–porphyrinic frameworks (MPFs) is appealing as these materials offer great opportunities for applications in artificial light-harvesting systems, gas storage, heterogeneous catalysis, etc. Herein, we report the synthesis of a novel mesoporous metal–porphyrinic framework (denoted as NUPF-1) and its catalytic properties. NUPF-1 is constructed from a new porphyrin linker and a  $Zr_6O_8$  structural building unit, possessing an unprecedented doubly interpenetrating **scu** net. The

structure exhibits not only remarkable chemical and thermal stabilities, but also a distinct structural flexibility, which is seldom seen in metal–organic framework (MOF) materials. By the merit of high chemical stability, NUPF-1 could be easily post-metallized with  $[Ru_3(CO)_{12}]$ , and the resulting {NUPF-1– $RuCO$ } is catalytically active as a heterogeneous catalyst for intermolecular  $C(sp^3)$ –H amination. Excellent yields and good recyclability for amination of small substrates with various organic azides have been achieved.

## Introduction

Metal–porphyrinic frameworks (MPFs), which contain (metallo)porphyrin-decorated ligands as linkers, are a subclass of metal–organic frameworks (MOFs).<sup>[1]</sup> Since the first report in the early 1990s,<sup>[2]</sup> MPFs have attracted escalating research interest owing to the unique electronic, chemical, and physical properties of the (metallo)porphyrins. In recent years, an increasing number of MPFs have been elaborately fabricated and exhibited fascinating chemical/physical properties, which made them eligible candidates for artificial light-harvesting systems,<sup>[3]</sup> gas storage/separation,<sup>[4]</sup> sensing,<sup>[5]</sup> photodynamic therapy,<sup>[6]</sup> catalysis,<sup>[7]</sup> etc. Nonetheless, the development of MPFs is still in its infancy. The total number of MPFs is rather small given the vast family of MOFs and the applications of MPFs remain largely unexplored.<sup>[8]</sup> Therefore, the exploration of novel porphyrinic building blocks and the underlying MPFs structures as well as their potential applications are still highly desirable.<sup>[9]</sup>

In pursuing MPFs, those with high chemical and thermal stabilities are much more appealing as these materials could not only diversify the applications of MPFs when subjected to harsh experimental environments,<sup>[7]</sup> but also provide a robust platform for further post modification/functionalization.<sup>[10]</sup> Thanks to its high charge density,  $Zr^{IV}$  can coordinate to the carboxylate groups of the ligand to form MOFs with extraordinarily high chemical and thermal stabilities.<sup>[11]</sup> By adopting this

strategy, many stable Zr-MPFs have been constructed, which have greatly promoted the development of MPFs.<sup>[4e,5a,7c,f,j,12]</sup> Meanwhile, it is believed that the central metal of the porphyrin units in MPFs play a vital role in its properties.<sup>[7]</sup> For example, MMPF-5(Cd) has a low catalytic activity toward epoxidation of *trans*-stilbene, but replacing  $Cd^{2+}$  by  $Co^{2+}$  in MMPF-5 drastically improved its catalytic performance.<sup>[13]</sup> Although the central porphyrin sites of MPFs are essential for catalysis, these sites can be easily blocked by metal coordination during the hydrothermal synthesis, which make MPFs inefficient for catalysis.<sup>[4a,7b,14]</sup> More importantly, for some metalloporphyrin-catalyzed reactions,<sup>[15]</sup> the catalytically-active metalloporphyrin centers are sensitive to water, oxygen, or other coordinating solvents, which would be destroyed in the MPFs synthesis process. Therefore, such reactions have rarely been explored using MPFs as the catalyst. To develop the applications of MPFs as catalysts for such reactions, the catalytic sites can only be made by post-metallation of the core-free MPFs. Because of the high oxophilicity,  $Zr^{IV}$  prefers to form Zr–O clusters rather than in-situ metallizing the porphyrin core during the solvothermal synthesis,<sup>[12a,16]</sup> which leads to core-free Zr-MPFs. The resulting core-free Zr-MPFs could be facilely post-metallized by various metals, imparting their multifunctionality.<sup>[4e,7f,12a,17]</sup> Therefore, in addition to the apparent desirable stability, the core-free nature of Zr-MPFs makes them versatile platforms for various applications.

One major motivation for constructing MPFs is their unique catalytic properties in heterogeneous catalysis. The use of MPFs as heterogeneous catalysts could not only overcome the drawbacks of separation and re-utilization of porphyrin molecules in homogeneous catalysis,<sup>[14,18]</sup> but also make the catalytically active porphyrinic units highly dispersed and accessible, overcoming the solubility issue that homogeneous porphyrinic catalysts often encounter,<sup>[7]</sup> thus resulting in superior catalytic performance. Recently, metalloporphyrins have been found to exhibit good catalytic activities for both intramolecular and intermolecular C–H aminations, which has attracted tremendous research interest.<sup>[19]</sup> However, these reactions were performed in homogeneous solutions, which cause problems for product purification and catalyst recycling. The latter has long been an aspiration because of the synthetic difficulties related to (metallo)porphyrins.<sup>[19c,20]</sup> Immobilizing the active sites of metalloporphyrins onto the pore surfaces of stable MPFs, that is, use of porous MPFs as heterogeneous catalysts for C–H amination,

[a] L. Xu, L. Sun, Z.-S. Cai, Prof. H.-B. Du  
State Key Laboratory of Coordination Chemistry  
Collaborative Innovation Center of Chemistry for Life Sciences  
School of Chemistry and Chemical Engineering  
Nanjing University, Nanjing, 210023 (P. R. China)  
E-mail: hbdu@nju.edu.cn

[b] Y.-P. Luo, Prof. M. Fang, Prof. R.-X. Yuan  
School of Chemistry and Materials Science  
Nanjing Normal University, Nanjing, 210023 (P. R. China)  
E-mail: fangmin@njjnu.edu.cn

[c] Prof. Y. Xu  
College of Chemistry and Chemical Engineering  
State Key Laboratory of Materials-Oriented Chemical Engineering  
Nanjing Tech University, Nanjing, 210009 (P. R. China)

[d] Prof. R.-X. Yuan  
School of Chemistry and Materials Engineering  
Changshu Institute of Technology, Changshu, 215500 (P. R. China)

Supporting information for this article is available on the WWW under <http://dx.doi.org/10.1002/chem.201600447>.

would address the issues of product purification and catalyst recycling. However, previous attempts to construct MPFs with large pores for this purpose have not been successful.<sup>[21]</sup> Herein, we report the synthesis of a novel mesoporous, core-free Zr-MPF, denoted as NUPF-1 (NUPF: Nanjing University Porphyrinic Framework no. 1). NUPF-1 possesses exceptionally high chemical and thermal stabilities. After post-metallization with  $[\text{Ru}_3\text{CO}_{12}]$ ,  $\{\text{NUPF-1-RuCO}\}$  acted as a heterogeneous catalyst for intermolecular  $\text{C}(\text{sp}^3)\text{-H}$  amination, exhibiting good catalytic performance and recyclability.

## Results and Discussion

Dark-purple rod-like single crystals of NUPF-1 were obtained by solvothermal reactions of a novel porphyrin ligand  $\text{H}_4\text{L}$  (Figure 1a) with  $\text{ZrOCl}_2 \cdot 8\text{H}_2\text{O}$  in DMF and formic acid at  $120^\circ\text{C}$  for 48 h (see the Supporting Information, Sections S2 and S3). Single-crystal X-ray diffraction studies revealed that NUPF-1 crystallizes in the orthorhombic  $Cmcm$  space group. As shown in Figure 1a, the porphyrin ligand in NUPF-1 is comprised of a tetraphenylporphyrin and benzoic acid moieties linked by amido units, with a span of  $\approx 2.4$  nm between the two neighboring carboxylate groups. The porphyrin macrocycle is core-free and almost planar with a maximum out-of-plane deformation of  $0.071 \text{ \AA}$ . The two phenyl rings in each of its arms tilt away from the porphyrin macrocycle with dihedral angles of  $72.1^\circ$  and  $49.9^\circ$  or  $80.1^\circ$  and  $57.1^\circ$ , respectively.  $\text{Zr}^{\text{IV}}$  forms an eight-connected  $\text{Zr}_6\text{O}_8$  structural building unit (SBU) (Figure 1b), similar to those found in PCN-225,<sup>[5a]</sup> but different to the commonly observed 12-connected  $\text{Zr}_6\text{O}_8$  cluster in the

UiO series.<sup>[11a]</sup> Each  $\text{Zr}_6\text{O}_8$  SBU in NUPF-1 is in a cuboid coordination geometry, connected by eight porphyrin ligands, while each porphyrin ligand is coordinated to four  $\text{Zr}_6\text{O}_8$  SBUs through its carboxylate groups. The linkage of the elongated porphyrin ligands and  $\text{Zr}_6\text{O}_8$  SBUs leads to a highly opened three-dimensional (4,8)- $\text{scu}$  net with very large rhombic channels of  $\approx 5.1 \times 2.3$  nm (atom-to-atom distance) running along the  $c$  axis. Interestingly, the  $\text{scu}$  net in NUPF-1 is doubly interpenetrated, which is unprecedented. An empirical pattern is that interpenetration often occurs to topologies with lower connectivity, and a framework with connectivity larger than six should not encounter interpenetration.<sup>[22]</sup> However, the voids in NUPF-1 are large enough to accommodate another individual network, resulting in an unprecedented twofold interpenetrating  $\text{scu}$  net (see the Supporting Information, Section S5). The interpenetration partitions each large rhombic channel into four smaller ones with the window sizes of  $2.66 \times 1.78$  nm,  $2.00 \times 0.72$  nm, and  $1.91 \times 0.67$  nm (Figure 1c and d). The calculated solvent-accessible pore volume is 73.6% of the unit cell volume (Figure S5 in the Supporting Information).<sup>[23]</sup>

NUPF-1 exhibits both high chemical and thermal stabilities. After the crystals of NUPF-1 were immersed into common organic solvents, boiling water, HCl (pH 1, 2, 3; 1 M and concentrated), and NaOH solutions (pH 9 and 10) for three days, all the samples except those in pH 10 solutions retained their crystallinity and morphology, as shown by powder XRD and optical images (Figure 2 and Figure S9a in the Supporting Information). The durability of NUPF-1 against acid is outstanding, and to the best of our knowledge, NUPF-1 is one of the rare MOFs that could resist concentrated HCl.<sup>[24]</sup> Even in aqua

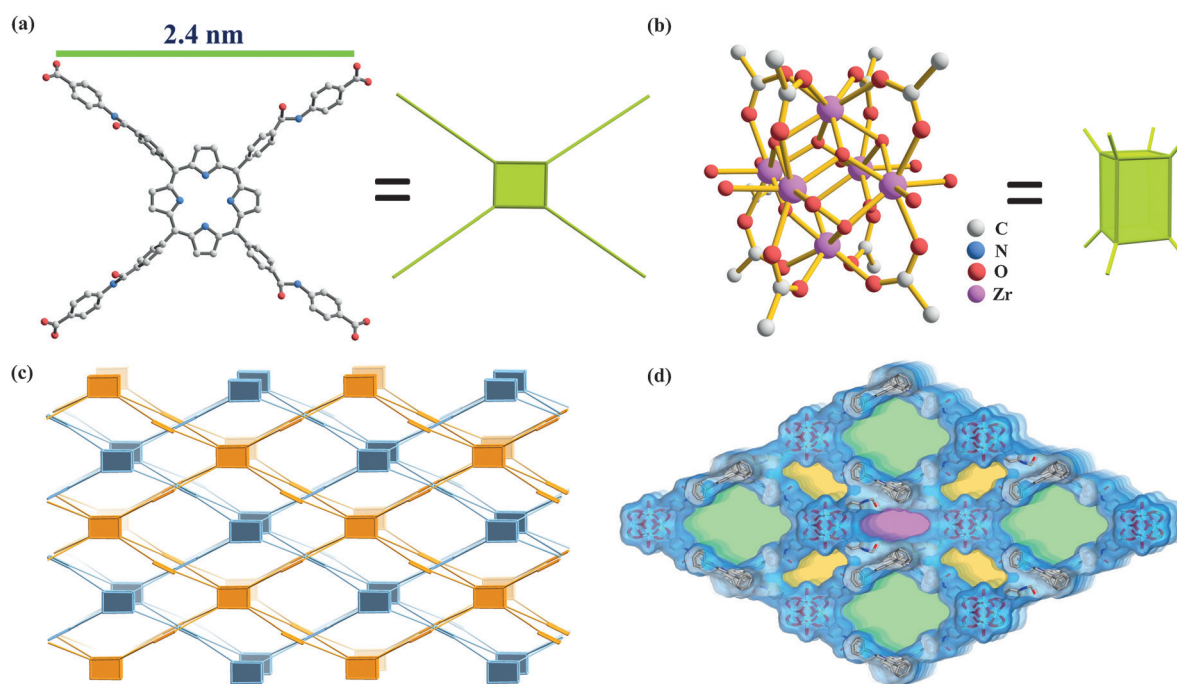


**Figure 1.** a) The square porphyrin carboxylate ligand in NUPF-1. b) The eight-connected  $\text{Zr}_6(\mu_3\text{-O})_4(\mu_3\text{-OH})_4(\text{OH})_4(\text{H}_2\text{O})_4(\text{OOC})_8$  SBU in NUPF-1. c) The two-fold interpenetrating  $\text{scu}$  framework of NUPF-1. d) Large channels of  $2.66 \times 1.78$  nm (green),  $2.00 \times 0.72$  nm (orange), and  $1.91 \times 0.67$  nm (pink) in NUPF-1 viewed along the  $c$  axis. The Connolly surfaces were calculated by using a  $1.4 \text{ \AA}$  probe radius.

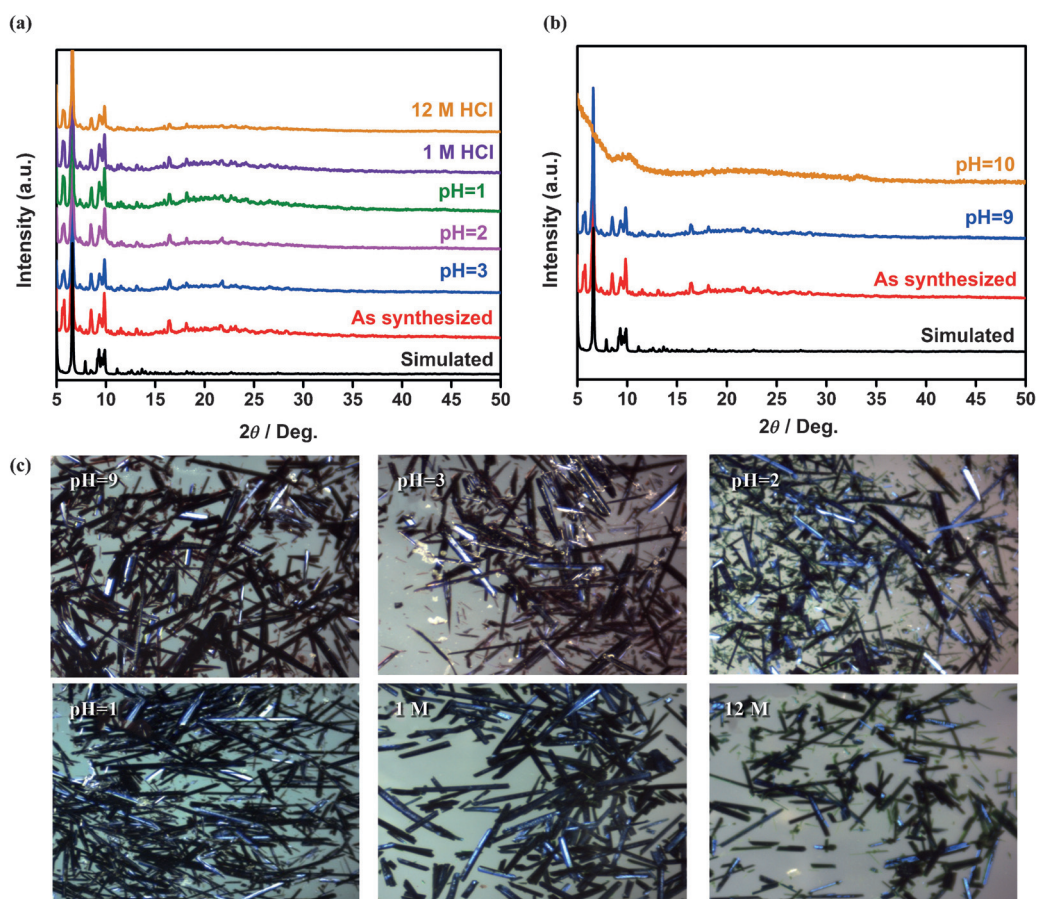


**Figure 2.** PXRD patterns of NUPF-1 soaked in different concentrations of a) HCl solutions and b) NaOH solutions for three days. The diffraction peak at  $2\theta = 5.71$  belongs to the (200) peak of NUPF-1, which was not evident in the calculated pattern. c) Optical images of NUPF-1 after soaking in acidic or alkaline solutions for three days.

regia, the crystalline structure of NUPF-1 could be maintained for 24 h (Figure S9b), further demonstrating its remarkable acid resistance. Thermogravimetric (TG) analysis (Figure S10a in the Supporting Information) and PXRD studies (Figure S10b) revealed that NUPF-1 was stable up to  $\sim 450^\circ\text{C}$ , demonstrating its high thermal stability. Moreover, NUPF-1 retained its crystallinity after exposure to  $12.5 \text{ tons cm}^{-2}$  of uniaxial pressure (Figure S11 in the Supporting Information), suggesting that it possesses excellent mechanical stability. The unusual structural stability of NUPF-1 laid the foundation for further exploration of its applications.

Interestingly, the porous NUPF-1 shows negligible  $\text{N}_2$  adsorption. PXRD analyses revealed that the structure was not decomposed after the adsorption measurements (Figure S12 in the Supporting Information). Many attempts to acquire large  $\text{N}_2$  adsorption have not been successful (see the Supporting Information, Section S13). The limited  $\text{N}_2$  adsorption is likely due to the low affinity of the NUPF-1 framework toward  $\text{N}_2$ , similar to other reported porous MPFs such as UNLPF-1 or ZnMn-RPM, etc., which have potential solvent-accessible volumes but no  $\text{N}_2$  uptake is seen with them.<sup>[4a,c,7b,25]</sup> Alternatively, for many MPFs, such as ZJU-18, CZJ-1, CZJ-4, etc., substrate adsorption has been used to probe their pore volumes.<sup>[7e,14,26]</sup> To probe the pores of NUPF-1, ethylbenzene adsorption was conducted

and analyzed by GC-MS with triphenylmethane as an internal standard. The results show that the adsorption capacities of the as-synthesized NUPF-1, and those treated with concentrated HCl and pH 9 solution were almost the same ( $\approx 32$  ethylbenzene per formula unit, see the Supporting Information, Section S13), indicating that the voids of NUPF-1 were preserved under harsh conditions. Indeed, as shown in Figure 3 a–c, the activated NUPF-1 could absorb  $107$ ,  $154$ , and  $182 \text{ cm}^3 \text{ g}^{-1}$  (STP) of ethanol, methanol, and water vapor, respectively, at 298 K and 1 atm. The samples treated with concentrated HCl absorbed  $119$ ,  $174$ , and  $280 \text{ cm}^3 \text{ g}^{-1}$  (STP) of ethanol, methanol, and water under the same conditions increased by a factor of 11.2%, 13.0%, and 53.8% compared with the as-synthesized sample, respectively. The enhancement in the adsorption by the HCl-treated sample may be ascribed to the removal of trace amount of trapped ligands in NUPF-1, which made the structure more open and thus improved the adsorption capacity.<sup>[7g]</sup> It is also possible that part of the amino or pyrrole moieties in NUPF-1 might be protonated in concentrated HCl solution, which could make the framework cationic and increase the affinity of NUPF-1 toward adsorbates.<sup>[5a,27]</sup> Notably, all the adsorption/desorption isotherms of ethanol, methanol, and water vapor over NUPF-1 showed unusually large desorption hysteresis loops. Such phenomenon have been found in flexi-

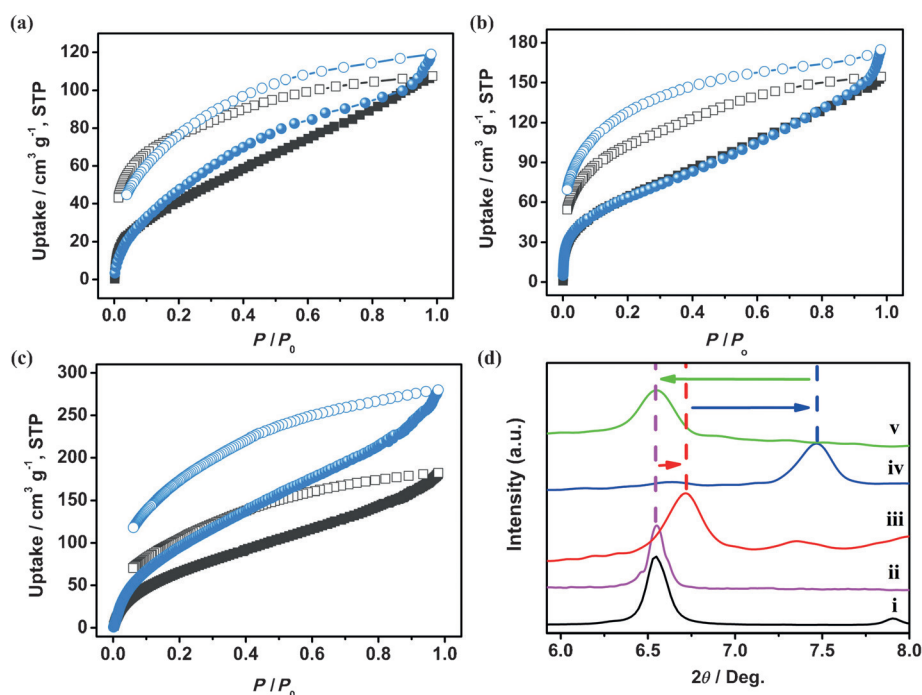


**Figure 3.** Adsorption (solid symbols) and desorption (open symbols) isotherms of activated NUPF-1 (squares) and HCl-treated NUPF-1 (circles) for: a) ethanol, b) methanol, and c) water. d) Powder XRD patterns of NUPF-1: (i) simulated based on crystal structure, (ii) pristine sample, (iii) evacuated at room temperature, (iv) heated at 450 °C under vacuum, and (v) heated at 450 °C and then soaked in DMF for 8 h.

ble MOFs,<sup>[28]</sup> suggesting that the highly stable NUPF-1 framework may exhibit some flexibility.

To verify this hypothesis, in situ variable-temperature X-ray diffraction (VT-XRD) measurements were conducted. Impressively, the flexibility of NUPF-1 was distinctly evident from the VT-XRD patterns. When the temperature gradually increased to 450 °C under vacuum, the main diffraction peak of NUPF-1 was maintained, confirming the high thermal stability (Figure S15a in the Supporting Information). However, upon evacuation at room temperature, the (220) diffraction peak of the pristine NUPF-1 at around 6.59° (2θ) shifted to a Bragg angle of 6.76° (2θ), indicating that solvent extraction induced a structural shrinkage (Figure 3d).<sup>[29]</sup> As the sample was heated up, the (220) peak sequentially moved to higher Bragg angles, up to 7.52° (2θ) at 450 °C (Figure S15b). These results demonstrate that the framework of NUPF-1 contracted upon evacuation or heating. Interestingly, the contracted framework of NUPF-1 could reversibly transfer back to the initial structure upon soaking the sample in DMF or EtOH. It is noted that only a few Zr-MOFs with high chemical and thermal stabilities accompanied by evident structural flexibility have been reported so far.<sup>[30]</sup> Recently, Hupp et al. reported the core-free Zr-MPF, NU-1104(H<sub>2</sub>), could undergo a structural transformation triggered by gas adsorption.<sup>[30b]</sup> The flexibility of NU-1104(H<sub>2</sub>) was attributed to the conformational changes in the core-free porphyrin linkers. Metallization of the porphyrin linkers in NU-1104 suppressed such flexibility. To check out whether metallization could eliminate the flexibility of NUPF-1, we prepared the metallized NUPF-1 with Ni, similar to NU-1104 (see the Supporting Information, Section S15).<sup>[4e]</sup> In contrast to NU-1104, in situ VT-

XRD measurements show that NUPF-1-Ni was still flexible, indicating metallization did not affect the flexibility of NUPF-1. The flexible nature of NUPF-1 likely arises from the interpenetration of the two extra-large-pored scu nets and the semi-rigid porphyrinic carboxylate ligand. The resulting highly porous NUPF-1 in its pristine form was swollen by guest solvents. The removal of guest solvents upon evacuation or heating would lead to sliding between the two interpenetrated nets and thus contraction of the framework.<sup>[28b,31]</sup> Meanwhile, the amido units in the elongated porphyrin ligands were flexible, which may twist under external stimuli, leading to the framework flexibility.<sup>[32]</sup>

Considering that most catalytic reactions are carried out in solvents,<sup>[33]</sup> and its high chemical stability, mesoporosity, and porphyrin core-free nature, NUPF-1 may be used as a versatile platform for heterogeneous catalysis. Among the metalloporphyrin-catalyzed reactions, intermolecular C(sp<sup>3</sup>)-H amination is an attractive but challenging one.<sup>[19]</sup> To explore the use of NUPF-1 in intermolecular C(sp<sup>3</sup>)-H amination, the {RuCO} units of the metalloporphyrins, which are sensitive to water and other coordinating solvents<sup>[34]</sup> and cannot be pre-planted or in situ metallized during the MPFs synthesis, were inserted into the free porphyrin core by post-metallization. The metallization process was easily accomplished by heating the archetypal crystals of NUPF-1 with [Ru<sub>3</sub>(CO)<sub>12</sub>] under reflux and a subsequent filtration operation, which bypassed the laborious chromatography purification process encountered in homogeneous catalyst preparation (see the Supporting Information, Section S16). The resulting {NUPF-1-RuCO} also exhibited high chemical/thermal stabilities, which were inherited from its

parent structure NUPF-1 (see the Supporting Information, Section S16). Such desirable stabilities would be beneficial for the further heterogeneous catalytic explorations.

Amination of ethylbenzene with *p*-nitrophenyl azide was chosen to evaluate the catalytic performance of {NUPF-1–RuCO}. As listed in Table 1, compared with the trials with the blank, the pristine NUPF-1, and [Ru<sub>3</sub>CO<sub>12</sub>] catalysts (entries 1, 2, and 3), {NUPF-1–RuCO} unequivocally exhibited catalytic activity toward ethylbenzene C(sp<sup>3</sup>)–H amination (entry 4). The yield is 94%, higher than that of the homogeneous catalyst [(tpp)RuCO] (≈73%, entry 5) under the same conditions (c.f.

80% with 8 mmol% catalyst loading reported in the literature).<sup>[35]</sup> Catalyst recycling tests revealed that {NUPF-1–RuCO} can be easily separated and re-used for further ethylbenzene amination, showing the advantages of a heterogeneous catalyst. Good yields of 89% and 84% were obtained in the 2nd and 3rd runs, respectively (entries 6 and 7). In addition, the crystalline nature of {NUPF-1–RuCO} was retained after the 3rd catalytic cycle (Figure S19 in the Supporting Information). The slight deactivation compared with the previous run is likely due to the exposure of the catalyst to water, oxygen, or other coordinating solvents during the handling, which destroyed some of the catalytically active intermediates.<sup>[34]</sup>

To further explore the catalytic performance of {NUPF-1–RuCO}, more azidobenzenes with different functional groups (entries 8–14) were used to aminate ethylbenzene. The catalytic results show that excellent yields of 72–89% have been achieved. The excellent catalytic performance of {NUPF-1–RuCO} may be attributed to the good dispersion of catalytic centers in the mesoporous NUPF-1, which resulted in effective utilization of the active sites.<sup>[7]</sup> In fact, MPFs as heterogeneous catalysts can, in many cases,<sup>[7a,d,13,36]</sup> generate higher catalytic yields than their counterparts in homogeneous catalysis. Moreover, {NUPF-1–RuCO} was shown not only to be catalytically active toward aryl azides, but also active in the reactions between ethylbenzene and sulfonyl or acyl azides to form aminated compounds with good yields of 83% and 72%, respectively (entries 15–16), demonstrating a good catalytic competence.

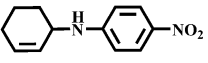
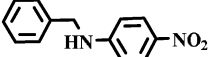
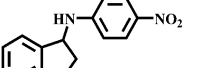
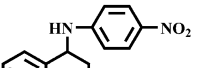
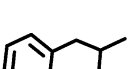
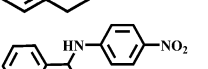
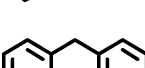
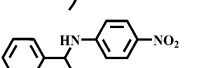
Similar to other heterogeneous reactions catalyzed by MOFs,<sup>[37]</sup> a slower conversion rate was observed in the amination of ethylbenzene with *p*-nitrophenyl azide catalyzed by {NUPF-1–RuCO}. Time-course plots reveal that full consumption of the azide needed nearly 18 h (see the Supporting Information, Section S20), whereas the same reaction catalyzed by [(tpp)RuCO] was accomplished in 5 h (Table 1, entry 5). These results indicate that the catalytic reaction occurred in the channels of {NUPF-1–RuCO} rather than on the external surface, as substrate-diffusion processes may be the bottleneck for the {NUPF-1–RuCO}-catalyzed reaction. To verify this, a “standard protocol” that gradually increased the size of substrates was followed.<sup>[33,38]</sup> If the catalysis indeed occurs mainly inside the pores of MOFs rather than on the surface, no or slow conversion of large substrates would be encountered. As shown in Table 2, the yields indeed gradually dropped with increasing size of the substrates. For example, an excellent yield of 93% was achieved in the amination of cyclohexene, whereas the yield decreased to 53% for 1,2,3,4-tetrahydronaphthalene. A low yield of 17% was observed for diphenylmethane, even with a prolonged reaction time. The exception was toluene, which has a smaller size but gave a good yield of 77.6% (Table 2, entry 2); this could be attributed to the un-

**Table 1.** Amination of ethylbenzene with various azides.

Entry	Azide	Catalyst	Product	Yield [%]
1		blank		0 <sup>[a]</sup>
2		NUPF-1		0 <sup>[a]</sup>
3		[Ru <sub>3</sub> CO <sub>12</sub> ]		6 <sup>[a]</sup>
4		{NUPF-1–RuCO}		94 <sup>[a]</sup>
5		[(tpp)RuCO]		73 <sup>[a,b]</sup>
6		{NUPF-1–RuCO}		89 (2nd run) <sup>[a]</sup>
7		{NUPF-1–RuCO}		84 (3rd run) <sup>[a]</sup>
8		{NUPF-1–RuCO}		87 <sup>[c]</sup>
9		{NUPF-1–RuCO}		72 <sup>[c]</sup>
10		{NUPF-1–RuCO}		87 <sup>[c]</sup>
11		{NUPF-1–RuCO}		87 <sup>[c]</sup>
12		{NUPF-1–RuCO}		85 <sup>[c]</sup>
13		{NUPF-1–RuCO}		89 <sup>[c]</sup>
14		{NUPF-1–RuCO}		78 <sup>[c]</sup>
15		{NUPF-1–RuCO}		83 <sup>[c]</sup>
16		{NUPF-1–RuCO}		72 <sup>[c]</sup>

Reactions were run under a high-purity Ar atmosphere with 3.0 mL of substrate, 0.3 mmol of azide, and 6 mmol% catalyst at 100 °C for 24 h unless stated otherwise.  
[a] Yield determined by <sup>1</sup>H NMR with 2,4-dinitrotoluene as the internal standard.  
[b] Reaction time = 5 h. [c] Isolated yield.

**Table 2.** Amination of various substrates with *p*-nitrophenyl azide.

Entry	Substrate	Catalyst	Product	Yield [%]
1		{NUPF-1-RuCO}		93 <sup>[a]</sup>
2		{NUPF-1-RuCO}		77.6 <sup>[a]</sup>
4		{NUPF-1-RuCO}		69 <sup>[b]</sup>
5		{NUPF-1-RuCO}		53 <sup>[b]</sup>
6		{NUPF-1-RuCO}		31 <sup>[b,c]</sup>
7		{NUPF-1-RuCO}		17 <sup>[b,c]</sup>

Reactions were run under a high-purity Ar atmosphere with 3.0 mL of substrate, 0.3 mmol of *p*-nitrophenyl azide, and 6 mmol% catalyst at 100 °C for 24 h unless stated otherwise. [a] Yield determined by <sup>1</sup>H NMR with 2,4-dinitrotoluene as the internal standard. [b] Isolated yield. [c] Reaction time = 48 h.

desired conversion of toluene to byproducts.<sup>[35]</sup> These results clearly prove that the catalytic reactions indeed occur in the internal pores of {NUPF-1-RuCO}.

It has been proposed that the metalloporphyrin-catalyzed intermolecular C–H amination requires the coordination of the ArN<sub>3</sub> moiety to the metal site to generate an active metal-imido complex.<sup>[19e]</sup> When a hydrocarbon substrate subsequently approaches to the active center, the nitrene transfer reaction takes place to form the adductive product. For {NUPF-1-RuCO}-catalyzed intermolecular C–H amination, the reaction occurs when the organic substrates and aryl azides effectively diffuse into the pores and approach the active metal sites. Meanwhile, the formed bulky products must diffuse out of the pores to regenerate the metal catalytic centers and make room for incoming substrates. The relatively large sizes of the molecules involved in the reactions likely resulted in diffusion bottlenecks during the {NUPF-1-RuCO}-catalyzed heterogeneous C(sp<sup>3</sup>)-H aminations, resulting in the characteristic slow conversion and shape selective catalysis.

## Conclusion

A new mesoporous zirconium-based metal-porphyrinic framework, named NUPF-1, has been synthesized, which possesses an unprecedented doubly interpenetrated *scu* framework. NUPF-1 not only exhibits remarkably high chemical and thermal stabilities, but also possesses a distinct structural flexibility. The flexibility likely originates from the interpenetration of the two large-pored *scu* nets and the flexible amido ligands.

NUPF-1 with large pores and desired chemical and thermal stabilities provides an ideal platform for heterogeneous catalysis. After post-metallization, {NUPF-1-RuCO} exhibits excellent, size-selective catalytic performance and good recyclability as a heterogeneous catalyst for intermolecular C(sp<sup>3</sup>)-H amination of small substrates with various organic azides. The unique structural features and properties of NUPF-1 will make it a promising candidate for a variety of applications.

## Experimental Section

### Synthesis of NUPF-1

Porphyrin ligand H<sub>4</sub>L (13 mg, 0.01 mmol) was transferred into *N,N*-dimethylformamide (DMF, 2 mL) in a small capped vial and sonicated for 10 min for dissolution. ZrOCl<sub>2</sub>·8H<sub>2</sub>O (10 mg, 0.03 mmol) and anhydrous formic acid (0.3 mL) were then added to the resulting solution and further sonicated for 10 min. The vial was placed into a Teflon-lined acid-digestion bomb and heated at 120 °C for 2 days and then allowed to cool to room temperature naturally. Small dark-purple rod-like crystals (Figure S3 in the Supporting Information) were harvested: yield ≈ 12 mg (≈ 72%, based on porphyrin ligand).

**Crystal data for NUPF-1:** C<sub>152</sub>H<sub>108</sub>N<sub>16</sub>O<sub>40</sub>Zr<sub>6</sub>, *M<sub>r</sub>* = 3345.86, dark-purple rod-like crystal, 0.15 × 0.13 × 0.12 mm<sup>3</sup>, orthorhombic, space group *Cmcm*, *a* = 30.6210(7) Å, *b* = 55.6255(9) Å, *c* = 24.4120(4) Å, α = β = γ = 90°, *V* = 41 581.2(13) Å<sup>3</sup>, *Z* = 4, ρ<sub>calcd</sub> = 0.534 g cm<sup>-3</sup>, *F*<sub>000</sub> = 6768, 57 649 reflections collected, 16 888 unique, (*R*<sub>int</sub> = 0.0779), final GooF = 1.056, *R*<sub>1</sub> = 0.0769, *wR*<sub>2</sub> = 0.2372. CCDC 1058125 contains the supplementary crystallographic data for this paper. These data are provided free of charge by The Cambridge Crystallographic Data Centre.

### Post-metallation of NUPF-1 with [Ru<sub>3</sub>(CO)<sub>12</sub>]

Toluene was dried before use. Under an argon atmosphere, NUPF-1 (80 mg, 0.05 mmol) and [Ru<sub>3</sub>(CO)<sub>12</sub>] (60 mg, 0.09 mmol) were suspended in dry toluene (15 mL) and heated at reflux at 120 °C for 24 h with shaking at 220 rpm by using a thermo-shaker. After the reaction flask cooled down to room temperature, the resulting crystals were collected in a filter, and washed thoroughly with dry toluene. The obtained {NUPF-1-RuCO} was used immediately.

### Catalytic reactions

All the reactions were carried out in a high-purity Ar atmosphere by employing standard Schlenk techniques and vacuum-line manipulations. All glassware was dried in an oven at 120 °C prior to use. Organic azides were synthesized by following the reported methods (see the Supporting Information, Section S1). Liquid substrates were distilled over sodium/benzophenone or dried by 4 Å molecular sieves. For a typical catalysis, organic azide (0.3 mmol) and catalyst (6 mmol%), that is, 53 mg for {NUPF-1-RuCO}, 14 mg for [(tpp)RuCO] (tpp = dianion of tetraphenylporphyrin), 12 mg for [Ru<sub>3</sub>CO<sub>12</sub>], 30 mg for NUPF-1, were added to a Schlenk flask. The flask was evacuated and backfilled with high-purity Ar three times. The liquid substrate (3 mL) was then added by a syringe under an Ar stream. The resulting mixture was shaken at 220 rpm by a thermo-shaker and heated at 100 °C for a certain period. After

the reaction was complete, the mixture was allowed to cool down to room temperature and the catalyst was isolated by centrifugation. The solution was concentrated to dryness, then  $\text{CHCl}_3$  (3 mL) was added to redissolve the residue. 2,4-Dinitrotoluene (0.1 mmol) was added to 1 mL of the above solution as a  $^1\text{H}$  NMR internal standard. The resulting solution was concentrated to dryness for the  $^1\text{H}$  NMR test. The remaining 2 mL of the above solution was purified by flash chromatography. For the high boiling point substrates, the solution was purified by silica gel column chromatography to give the corresponding products.

Other experimental details and characterizations are given in the Supporting Information.

## Acknowledgments

The authors are grateful for financial support from the National Natural Science Foundation of China (grant number 21471075).

**Keywords:** heterogeneous catalysis • mesoporous materials • metal–organic frameworks • zirconium

- [1] a) H.-C. Zhou, J. R. Long, O. M. Yaghi, *Chem. Rev.* **2012**, *112*, 673–674; b) H. C. Zhou, S. Kitagawa, *Chem. Soc. Rev.* **2014**, *43*, 5415–5418.
- [2] B. F. Abrahams, B. F. Hoskins, R. Robson, *J. Am. Chem. Soc.* **1991**, *113*, 3606–3607.
- [3] a) C. Y. Lee, O. K. Farha, B. J. Hong, A. A. Sarjeant, S. T. Nguyen, J. T. Hupp, *J. Am. Chem. Soc.* **2011**, *133*, 15858–15861; b) A. Fateeva, P. A. Chater, C. P. Ireland, A. A. Tahir, Y. Z. Khimiyak, P. V. Wiper, J. R. Darwent, M. J. Rosseinsky, *Angew. Chem. Int. Ed.* **2012**, *51*, 7440–7444; *Angew. Chem.* **2012**, *124*, 7558–7562; c) H.-J. Son, S. Jin, S. Patwardhan, S. J. Wezenberg, N. C. Jeong, M. So, C. E. Wilmer, A. A. Sarjeant, G. C. Schatz, R. Q. Snurr, O. K. Farha, G. P. Wiederrecht, J. T. Hupp, *J. Am. Chem. Soc.* **2012**, *134*, 9537–9540; d) H.-Q. Xu, J. Hu, D. Wang, Z. Li, Q. Zhang, Y. Luo, S.-H. Yu, H.-L. Jiang, *J. Am. Chem. Soc.* **2015**, *137*, 13440–13443.
- [4] a) X.-S. Wang, L. Meng, Q. Cheng, C. Kim, L. Wojtas, M. Chrzanowski, Y.-S. Chen, X. P. Zhang, S. Ma, *J. Am. Chem. Soc.* **2011**, *133*, 16322–16325; b) X.-S. Wang, M. Chrzanowski, W.-Y. Gao, L. Wojtas, Y.-S. Chen, M. J. Zaworotko, S. Ma, *Chem. Sci.* **2012**, *3*, 2823–2827; c) J. A. Johnson, Q. Lin, L.-C. Wu, N. Obaidi, Z. L. Olson, T. C. Reeson, Y.-S. Chen, J. Zhang, *Chem. Commun.* **2013**, *49*, 2828–2830; d) Z. Guo, D. Yan, H. Wang, D. Tesfagaber, X. Li, Y. Chen, W. Huang, B. Chen, *Inorg. Chem.* **2014**, *53*, 200–204; e) T. C. Wang, W. Bury, D. A. Gómez-Gualdrón, N. A. Vermeulen, J. E. Mondloch, P. Deria, K. Zhang, P. Z. Moghadam, A. A. Sarjeant, R. Q. Snurr, J. F. Stoddart, J. T. Hupp, O. K. Farha, *J. Am. Chem. Soc.* **2015**, *137*, 3585–3591; f) O. T. Wilcox, A. Fateeva, A. P. Katsoulidis, M. W. Smith, C. A. Stone, M. J. Rosseinsky, *Chem. Commun.* **2015**, *51*, 14989–14991.
- [5] a) H.-L. Jiang, D. Feng, K. Wang, Z.-Y. Gu, Z. Wei, Y.-P. Chen, H.-C. Zhou, *J. Am. Chem. Soc.* **2013**, *135*, 13934–13938; b) B. J. Deibert, J. Li, *Chem. Commun.* **2014**, *50*, 9636–9639; c) J. Yang, Z. Wang, K. Hu, Y. Li, J. Feng, J. Shi, *J. Gu, ACS Appl. Mater. Interfaces* **2015**, *7*, 11956–11964.
- [6] K. Lu, C. He, W. Lin, *J. Am. Chem. Soc.* **2014**, *136*, 16712–16715.
- [7] a) A. M. Shultz, O. K. Farha, J. T. Hupp, S. T. Nguyen, *J. Am. Chem. Soc.* **2009**, *131*, 4204–4205; b) O. K. Farha, A. M. Shultz, A. A. Sarjeant, S. T. Nguyen, J. T. Hupp, *J. Am. Chem. Soc.* **2011**, *133*, 5652–5655; c) D. Feng, Z.-Y. Gu, J.-R. Li, H.-L. Jiang, Z. Wei, H.-C. Zhou, *Angew. Chem. Int. Ed.* **2012**, *51*, 10307–10310; *Angew. Chem.* **2012**, *124*, 10453–10456; d) L. Meng, Q. Cheng, C. Kim, W.-Y. Gao, L. Wojtas, Y.-S. Chen, M. J. Zaworotko, X. P. Zhang, S. Ma, *Angew. Chem. Int. Ed.* **2012**, *51*, 10082–10085; *Angew. Chem.* **2012**, *124*, 10229–10232; e) X.-L. Yang, M.-H. Xie, C. Zou, Y. He, B. Chen, M. O’Keeffe, C.-D. Wu, *J. Am. Chem. Soc.* **2012**, *134*, 10638–10645; f) D. Feng, W.-C. Chung, Z. Wei, Z.-Y. Gu, H.-L. Jiang, Y.-P. Chen, D. J. Darensbourg, H.-C. Zhou, *J. Am. Chem. Soc.* **2013**, *135*, 17105–17110; g) K. Wang, D. Feng, T.-F. Liu, J. Su, S. Yuan, Y.-P. Chen, M. Bosch, X. Zou, H.-C. Zhou, *J. Am. Chem. Soc.* **2014**, *136*, 13983–13986; h) M. Zhao, S. Ou, C.-D. Wu, *Acc. Chem. Res.* **2014**, *47*, 1199–1207; i) J. A. Johnson, X. Zhang, T. C. Reeson, Y.-S. Chen, J. Zhang, *J. Am. Chem. Soc.* **2014**, *136*, 15881–15884; j) D. Feng, Z.-Y. Gu, Y.-P. Chen, J. Park, Z. Wei, Y. Sun, M. Bosch, S. Yuan, H.-C. Zhou, *J. Am. Chem. Soc.* **2014**, *136*, 17714–17717; k) J. Zheng, M. Wu, F. Jiang, W. Su, M. Hong, *Chem. Sci.* **2015**, *6*, 3466–3470; l) N. Kornienko, Y. Zhao, C. S. Kley, C. Zhu, D. Kim, S. Lin, C. J. Chang, O. M. Yaghi, P. Yang, *J. Am. Chem. Soc.* **2015**, *137*, 14129–14135; m) T. Toyao, N. Ueno, K. Miyahara, Y. Matsui, T.-H. Kim, Y. Horiuchi, H. Ikeda, M. Matsuoka, *Chem. Commun.* **2015**, *51*, 16103–16106; n) J. A. Johnson, J. Luo, X. Zhang, Y.-S. Chen, M. D. Morton, E. Echeverría, F. E. Torres, J. Zhang, *ACS Catal.* **2015**, *5*, 5283–5291.
- [8] a) B. J. Burnett, P. M. Barron, W. Choe, *CrystEngComm* **2012**, *14*, 3839–3846; b) C. Zou, C.-D. Wu, *Dalton Trans.* **2012**, *41*, 3879–3888; c) W.-Y. Gao, M. Chrzanowski, S. Ma, *Chem. Soc. Rev.* **2014**, *43*, 5841–5866; d) Z. Guo, B. Chen, *Dalton Trans.* **2015**, *44*, 14574–14583.
- [9] Q. Lin, X. Bu, A. Kong, C. Mao, X. Zhao, F. Bu, P. Feng, *J. Am. Chem. Soc.* **2015**, *137*, 2235–2238.
- [10] K. Sasan, Q. Lin, C. Mao, P. Feng, *Chem. Commun.* **2014**, *50*, 10390–10393.
- [11] a) J. H. Cavka, S. Jakobsen, U. Olsbye, N. Guillou, C. Lamberti, S. Bordiga, K. P. Lillerud, *J. Am. Chem. Soc.* **2008**, *130*, 13850–13851; b) T. Devic, C. Serre, *Chem. Soc. Rev.* **2014**, *43*, 6097–6115.
- [12] a) W. Morris, B. Voloskiy, S. Demir, F. Gándara, P. L. McGrier, H. Furukawa, D. Cascio, J. F. Stoddart, O. M. Yaghi, *Inorg. Chem.* **2012**, *51*, 6443–6445; b) T.-F. Liu, D. Feng, Y.-P. Chen, L. Zou, M. Bosch, S. Yuan, Z. Wei, S. Fordham, K. Wang, H.-C. Zhou, *J. Am. Chem. Soc.* **2015**, *137*, 413–419.
- [13] X.-S. Wang, M. Chrzanowski, L. Wojtas, Y.-S. Chen, S. Ma, *Chem. Eur. J.* **2013**, *19*, 3297–3301.
- [14] X.-L. Yang, C.-D. Wu, *Inorg. Chem.* **2014**, *53*, 4797–4799.
- [15] a) C.-Y. Zhou, W.-Y. Yu, P. W. H. Chan, C.-M. Che, *J. Org. Chem.* **2004**, *69*, 7072–7082; b) R. Wakabayashi, T. Kurahashi, S. Matsubara, *Org. Lett.* **2012**, *14*, 4794–4797; c) P. Zardi, A. Caselli, P. Macchi, F. Ferretti, E. Gallo, *Organometallics* **2014**, *33*, 2210–2218.
- [16] H. J. Kim, D. Whang, K. Kim, Y. Do, *Inorg. Chem.* **1993**, *32*, 360–362.
- [17] a) I. Hod, M. D. Sampson, P. Deria, C. P. Kubiak, O. K. Farha, J. T. Hupp, *ACS Catal.* **2015**, *5*, 6302–6309; b) C.-W. Kung, T.-H. Chang, L.-Y. Chou, J. T. Hupp, O. K. Farha, K.-C. Ho, *Chem. Commun.* **2015**, *51*, 2414–2417.
- [18] Y. Liu, A. J. Howarth, J. T. Hupp, O. K. Farha, *Angew. Chem. Int. Ed.* **2015**, *54*, 9001–9005; *Angew. Chem.* **2015**, *127*, 9129–9133.
- [19] a) H. Lu, H. Jiang, L. Wojtas, X. P. Zhang, *Angew. Chem. Int. Ed.* **2010**, *49*, 10192–10196; *Angew. Chem.* **2010**, *122*, 10390–10394; b) C.-M. Che, V. K.-Y. Lo, C.-Y. Zhou, J.-S. Huang, *Chem. Soc. Rev.* **2011**, *40*, 1950–1975; c) H. Lu, X. P. Zhang, *Chem. Soc. Rev.* **2011**, *40*, 1899–1909; d) G. Tseberlidis, P. Zardi, A. Caselli, D. Cancogni, M. Fusari, L. Lay, E. Gallo, *Organometallics* **2015**, *34*, 3774–3781; e) D. Intriери, P. Zardi, A. Caselli, E. Gallo, *Chem. Commun.* **2014**, *50*, 11440–11453.
- [20] A. Ciammaichella, A. Leoni, P. Tagliatesta, *New J. Chem.* **2010**, *34*, 2122–2124.
- [21] L. Carlucci, G. Ciani, S. Maggini, D. M. Proserpio, F. Ragaini, E. Gallo, M. Rancocchiarri, A. Caselli, *J. Porphyrins Phthalocyanines* **2010**, *14*, 804–814.
- [22] M. Zhang, Y.-P. Chen, M. Bosch, T. Gentle, K. Wang, D. Feng, Z. U. Wang, H.-C. Zhou, *Angew. Chem. Int. Ed.* **2014**, *53*, 815–818; *Angew. Chem.* **2014**, *126*, 834–837.
- [23] A. L. Spek, *J. Appl. Crystallogr.* **2003**, *36*, 7–13.
- [24] S. Wang, J. Wang, W. Cheng, X. Yang, Z. Zhang, Y. Xu, H. Liu, Y. Wu, M. Fang, *Dalton Trans.* **2015**, *44*, 8049–8061.
- [25] a) L. Zhang, C. Wang, X. Zhao, F. Yu, F.-F. Yao, J. Li, *Inorg. Chem. Commun.* **2015**, *55*, 123–128; b) W.-Y. Gao, Z. Zhang, L. Cash, L. Wojtas, Y.-S. Chen, S. Ma, *CrystEngComm* **2013**, *15*, 9320–9323.
- [26] a) C. Zou, T. Zhang, M.-H. Xie, L. Yan, G.-Q. Kong, X.-L. Yang, A. Ma, C.-D. Wu, *Inorg. Chem.* **2013**, *52*, 3620–3626; b) W. Zhang, P. Jiang, Y. Wang, J. Zhang, J. Zheng, P. Zhang, *Chem. Eng. J.* **2014**, *257*, 28–35; c) M.-H. Xie, X.-L. Yang, Y. He, J. Zhang, B. Chen, C.-D. Wu, *Chem. Eur. J.* **2013**, *19*, 14316–14321.
- [27] X.-S. Wang, S. Ma, D. Sun, S. Parkin, H.-C. Zhou, *J. Am. Chem. Soc.* **2006**, *128*, 16474–16475.
- [28] a) C. Serre, C. Mellot-Draznieks, S. Surblé, N. Audebrand, Y. Filinchuk, G. Férey, *Science* **2007**, *315*, 1828–1831; b) T. K. Maji, R. Matsuda, S. Kitagawa, *Nat. Mater.* **2007**, *6*, 142–148; c) A. Shigematsu, T. Yamada, H. Kitagawa, *J. Am. Chem. Soc.* **2011**, *133*, 2034–2036.
- [29] S. Henke, A. Schneemann, A. Wütscher, R. A. Fischer, *J. Am. Chem. Soc.* **2012**, *134*, 9464–9474.

- [30] a) Q. Zhang, J. Su, D. Feng, Z. Wei, X. Zou, H.-C. Zhou, *J. Am. Chem. Soc.* **2015**, *137*, 10064–10067; b) P. Deria, D. A. Gómez-Gualdrón, W. Bury, H. T. Schaefer, T. C. Wang, P. K. Thallapally, A. A. Sarjeant, R. Q. Snurr, J. T. Hupp, O. K. Farha, *J. Am. Chem. Soc.* **2015**, *137*, 13183–13190.
- [31] a) S. Horike, S. Shimomura, S. Kitagawa, *Nat. Chem.* **2009**, *1*, 695–704; b) S. Bureekaew, H. Sato, R. Matsuda, Y. Kubota, R. Hirose, J. Kim, K. Kato, M. Takata, S. Kitagawa, *Angew. Chem. Int. Ed.* **2010**, *49*, 7660–7664; *Angew. Chem.* **2010**, *122*, 7826–7830; c) Y. Sakata, S. Furukawa, M. Kondo, K. Hirai, N. Horike, Y. Takashima, H. Uehara, N. Louvain, M. Meilikhov, T. Tsuruoka, S. Isoda, W. Kosaka, O. Sakata, S. Kitagawa, *Science* **2013**, *339*, 193–196.
- [32] A. Karmakar, A. V. Desai, B. Manna, B. Joarder, S. K. Ghosh, *Chem. Eur. J.* **2015**, *21*, 7071–7076.
- [33] M. Yoon, R. Srirambalaji, K. Kim, *Chem. Rev.* **2012**, *112*, 1196–1231.
- [34] S. Fantauzzi, E. Gallo, A. Caselli, F. Ragaini, N. Casati, P. Macchi, S. Cenini, *Chem. Commun.* **2009**, 3952–3954.
- [35] D. Intriери, A. Caselli, F. Ragaini, S. Cenini, E. Gallo, *J. Porphyrins Phthalocyanines* **2010**, *14*, 732–740.
- [36] Y. Chen, T. Hoang, S. Ma, *Inorg. Chem.* **2012**, *51*, 12600–12602.
- [37] a) J. S. Seo, D. Whang, H. Lee, S. I. Jun, J. Oh, Y. J. Jeon, K. Kim, *Nature* **2000**, *404*, 982–986; b) Y. K. Hwang, D.-Y. Hong, J.-S. Chang, S. H. Jhung, Y.-K. Seo, J. Kim, A. Vimont, M. Daturi, C. Serre, G. Férey, *Angew. Chem. Int. Ed.* **2008**, *47*, 4144–4148; *Angew. Chem.* **2008**, *120*, 4212–4216; c) A. Corma, H. Garcia, F. X. L. I. Xamena, *Chem. Rev.* **2010**, *110*, 4606–4655; d) I. Luz, F. X. Llabrés i Xamena, A. Corma, *J. Catal.* **2012**, *285*, 285–291.
- [38] A. Dhakshinamoorthy, H. Garcia, *Chem. Soc. Rev.* **2014**, *43*, 5750–5765.

---

Received: January 20, 2016

Published online on March 9, 2016